

CALCULATION AND EXPERIMENTAL RESEARCH OF STATIC AND DYNAMIC VOLT-AMPERE CHARACTERISTICS OF ARGON ARC WITH REFRACTORY CATHODE*

V.N. SYDORETS, I.V. KRIVTSUN, V.F. DEMCHENKO, I.V. KRIKENT,
D.V. KOVALENKO, I.V. KOVALENKO and A.G. PAVLOV

E.O. Paton Electric Welding Institute, NASU
11 Kazimir Malevich Str., 03680, Kiev, Ukraine. E-mail: office@paton.kiev.ua

Well-grounded selection of optimum modes of non-consumable pulse-arc welding requires investigation of dynamics of pulsed arc burning. Proposed earlier model of nonstationary arc with distributed parameters, due to large computing expenses, allows considering effect on arc of only single current pulse. Whereas, investigation of dynamic characteristics of the arc in supply of batches of high-frequency pulses of welding current is of practical interest. In this connection, it is interesting to develop an arc dynamic model with lumped parameters, which does not have limitations from point of view of amount of computations and allows high accuracy tracing of the dynamics of change of characteristics in arc with refractory cathode at high-frequency current modulation. The same data were received for comparison using calculation method based on the model with distributed parameters. Arc column time constant was determined based on calculation data of dynamics of arc voltage change, received employing the model with distributed parameters. In total complex of carried research and experimental investigations allowed working out an algorithms of application of the model with lumped parameters and identifying them. The results are given on experimental investigations of dynamics of change of current and arc voltage in high-frequency non-consumable pulse-arc welding, which are matched with the results of calculations using the model with lumped parameters. 14 Ref., 1 Table, 8 Figures.

Keywords: pulse-arc welding, non-consumable electrode welding, high-frequency pulses, dynamic characteristics of arc, nonstationary arc, arc column, argon arc, refractory cathode

Non-consumable inert gas arc (TIG) welding is widely used in manufacture of critical structures in nuclear and chemical machine building, aircraft and rocket construction, food and other branches of industry. The disadvantage of TIG welding is low efficiency promoted by insufficient penetration capability of the arc. In order to eliminate this disadvantage different methods of activation of processes of energy transfer in arc plasma and weld pool, namely welding over activating flux layer (A-TIG process) and hybrid welding (TIG + laser) etc., are currently used [1–4]. Work [5], employing the methods of mathematical modelling of arc with refractory cathode, states an effect of significant increase of current density at pulse leading edge and density of heat flow at anode in supply of welding current pulse with high rate of its change in comparison with corresponding characteristics of stationary arc. A technological consequence, which can be expected as a result of intensification of heat and dynamic impact of pulsed

arc on melt, can be an increase of penetration depth and rise of molten metal volume in comparison with direct current welding.

Indicated peculiarity of dynamics of arc burning in the pulse mode indicate that high-frequency modulation of welding current can be used as one more method for activation of processes of energy transfer in arc plasma and metal being welded at corresponding selection of mode parameters. This promotes for an interest in further investigations of dynamic characteristics of the arc with refractory cathode in pulse mode. The primary instrument, which is widely used in welding arc analysis, is its volt-ampere characteristic (VAC). Investigation of relationship between current and voltage in non-consumable electrode welding is of interest in the case of direct current welding as well as in the case of high-frequency current pulse modulation, at which described above dynamic processes are observed. Present work is dedicated to experimental and theoretical investigation of static and

*Based on materials presented on at VII International Conference «Mathematical Modelling and Information Technologies in Welding and Related Processes», September 15–19, 2014, Odessa, Ukraine.

dynamic VAC of the argon arc with refractory cathode.

The model of nonstationary arc, proposed in work [6] and realized in work [5], is based on description of processes of energy-, mass- and electric transfer in column plasma and anode area of the nonstationary arc with refractory cathode (model with distributed parameters). Such an approach requires significant computation resources for calculation of heat, electromagnetic and gas-dynamic characteristics of the arc plasma, that limits the field of model application by consideration of only single current pulses. At the same time, researching the effect of batches of pulses of different shape and frequency is of practical interest.

Main definitions. Relationship between current I and arc voltage U is set by determination of electric arc VAC. It is known fact that arc voltage is the sum of three constituents, namely cathode potential drop U_c , arc column voltage U_p and anode potential drop U_a , which is negative [7] for most of electric atmospheric pressure arcs, including for welding arcs. Since the potentials on the surface of metallic cathode and anode can be considered constant with sufficient accuracy (due to high electric conductivity of metals), a total arc voltage U can be determined (measured) as a difference of potentials of anode and cathode surface, i.e. it is assumed that $U = \varphi_a - \varphi_c$, where φ_a , φ_c are the potentials of working surfaces of anode and cathode, respectively. However, such generally accepted determination of voltage as integral electric characteristic of arc discharge is not acceptable for determination of its constituents, namely cathode U_c and anode U_a potential drop as well as arc column voltage U_p . It is caused by the fact that according to calculations of characteristics of plasma of argon arc with refractory cathode and water-cooled [8] or evaporating [9] anode, particularly, arc in hybrid (TIG + CO₂-laser) welding [10], plasma potential in the anode layer interface φ_{ap} , the same as plasma potential in the cathode layer interface φ_{cp} , vary along Γ_{ap} and Γ_{cp} interfaces, dividing the anode and cathode areas with arc column, i.e. specified conditions are not equipotential.

The following is done for determination of effective (integral) values of anode drop $\langle U_a \rangle$, which in sum with correspondingly determined values of cathode drop $\langle U_c \rangle$ and column voltage $\langle U_p \rangle$ shall provide the total arc voltage $U = \langle U_c \rangle + \langle U_p \rangle + \langle U_a \rangle$. The following integral relationship arises from equation of continuity $\text{div } \vec{j} = 0$, since density of electric current in the arc column is determined by expression $\vec{j} = -\sigma \text{grad } \varphi$, where σ is the electric conductivity, and φ is the potential of electric field in arc column plasma:

$$\int_{\Omega} \frac{|\vec{j}|^2}{\sigma} dV = - \int_{\Gamma} \varphi j_n dS, \quad (1)$$

where Ω is the area covered by arc column; Γ is its boundary; j_n is the projection of vector of current density to the external normal \vec{n} to boundary Γ . Boundary Γ is presented as $\Gamma = \Gamma_{ap} + \Gamma_{cp} + \Gamma_{bp}$, where Γ_{bp} is the part of boundary Γ without current ($j_n|_{\Gamma_{bp}} = 0$). Then, the following is received from (1):

$$\int_{\Omega} \frac{|\vec{j}|^2}{\sigma} dV = \int_{\Gamma_{ap}} \varphi j_{n'} d\Gamma_{ap} - \int_{\Gamma_{cp}} \varphi j_n d\Gamma_{cp}, \quad (2)$$

where $\vec{n}' = -\vec{n}$. Expression in the left part of (2) is the thermal power, emitted in the arc column.

The following is written in accordance with Joule-Lenz's law:

$$\int_{\Omega} \frac{|\vec{j}|^2}{\sigma} dV = I \langle U_p \rangle,$$

where under

$$\langle U_p \rangle = \frac{1}{I} \int_{\Omega} \frac{|\vec{j}|^2}{\sigma} dV$$

the effective arc column voltage drop should be realized. Since Γ_{ap} and Γ_{cp} surfaces are not equipotential, let's introduce for them the concepts of the effective values of potentials Φ_{ap} and Φ_{cp} in the following way

$$\Phi_{ap} = \frac{1}{I} \int_{\Gamma_{ap}} \varphi j_{n'} d\Gamma_{ap}; \quad \Phi_{cp} = \frac{1}{I} \int_{\Gamma_{cp}} \varphi j_n d\Gamma_{cp}. \quad (3)$$

Then proceeding from (2) the arc column voltage drop can be determined as a difference of the effective values of potentials Φ_{ap} and Φ_{cp} , i.e. assuming $\langle U_p \rangle = \Phi_{ap} - \Phi_{cp}$. Using (3), the effective anode $\langle U_a \rangle$ and cathode $\langle U_c \rangle$ drops are determined in form of

$$\langle U_a \rangle = \varphi_a - \Phi_{ap}; \quad \langle U_c \rangle = \Phi_{cp} - \varphi_c.$$

Standard expression for arc voltage in form of sum of voltage drops in separate segments of the arc discharge can be obtained in scope of given definitions:

$$U = \langle U_c \rangle + \langle U_p \rangle + \langle U_a \rangle = \varphi_a - \varphi_c, \quad (4)$$

where it should be taken into account that the effective anode voltage drop is negative.

Static VAC of argon arc with refractory cathode. Let's consider the results of experimental measurements of static VAC of arcs with $l = 1.5$ and 3.0 mm lengths, burning on water-cooled anode. Figure 1 provides for experimental data in form of separate markers, the hatches show approximation of these data by Laurent series, coefficients of which are presented in the Table:

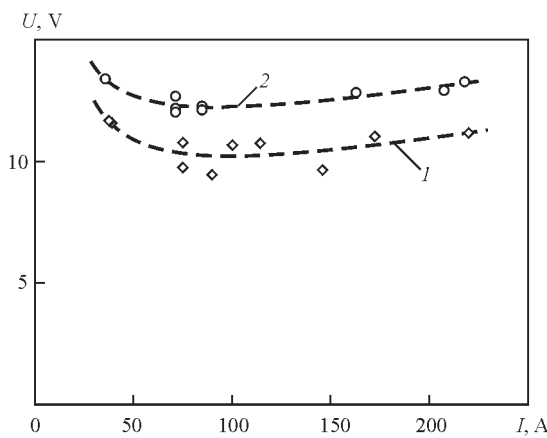
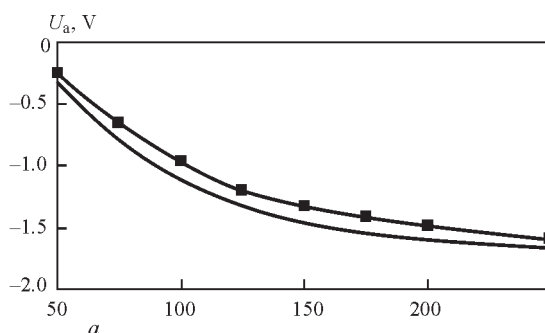


Figure 1. Experimental data and approximations of static VAC of 1.5 (1) and 3.0 mm (2) length argon arc with refractory cathode and copper water-cooled anode

$$U(I) = \sum_{j=-1}^{j=1} a_j \left(\frac{I}{100} \right)^j \quad (5)$$

Results of calculations in [8] for distributed characteristics of 3 mm length stationary arc, carried in $I = 50\text{--}250$ A current range, based on model of work [6], are used for theoretical evaluation of arc voltage constituents, being included in formula (4). Curves with markers from Figure 2 show dependence on arc current of anode potential drop $\langle U_a \rangle$ and total voltage on column and anode area of the arc $\langle U_{pa} \rangle = \langle U_p \rangle + \langle U_a \rangle$, calculated by difference of effective (integral) values of potentials on corresponding surfaces. The same Figure curves without markers show voltage drop U_{a0} , $U_{pa0} = U_{p0} + U_{a0}$ determined as difference of axial values of corresponding potentials. As follows from presented curves, an error in determination of the arc column voltage and potential drop in the anode layer, using two studied methods, is around 10%. However, the effective values, introduced in the first chapter of this work, will be used for further analysis and averaging sign $\langle \rangle$ is eliminated for their writing.

Model [6] does not consider cathode area of the arc in explicit form, therefore theoretical evaluation of values of the cathode potential drop using data of calculations, made in work [8], is not possible.



Coefficients of approximation

Arc length l , mm		1.5	3.0
Coefficient of approximation	a_{-1}	1.394283	1.113619
	a_0	7.343352	9.765307
	a_1	1.443792	1.333032

In order to find U_c let's use experimental data (see Figure 1) and calculate the cathode voltage drop as a difference between experimentally determined value U and calculated effective voltage on column and anode area of arc $U_{pa} = U_p + U_a$, given in Figure 3. Figure 4 shows determined in such a way change of the effective cathode drop U_c depending on arc current. The same Figure represents calculation data on value of the cathode voltage drop, from presentation [8], based on approximated model of cathode layer. Comparison of these results indicates qualitatively similar nature of dependence of cathode drop on current, however it is around 1.3 V variation of data. Obtained in such a way calculation-experimental data on $U_c(I)$ dependences (see curve 2 in Figure 4) will be used for determination of dynamic VAC of the pulsed arc.

Dynamic model of arc with lumped parameters. Equations of dynamic model of arc with lumped parameters, allowing analytical solution which is not related with intricate calculations, is developed as an alternative to nonstationary arc model with distributed parameters [5, 6].

The arc column in scope of given model is considered as some object following energy conservation law [12]

$$\frac{dQ}{dt} = P - P_\theta \quad (6)$$

where Q is the arc column internal energy; P , P_θ are the input and output power, respectively. Application of the arc column VAC $I_p^{st}(I)$ and corresponding time constant θ as initial data allows this model to describe the arc dynamics at any current change $I(t)$:

$$U_p(t) = \frac{U_p^{st}(i_\theta(t))}{i_\theta(t)} I(t) \quad (7)$$

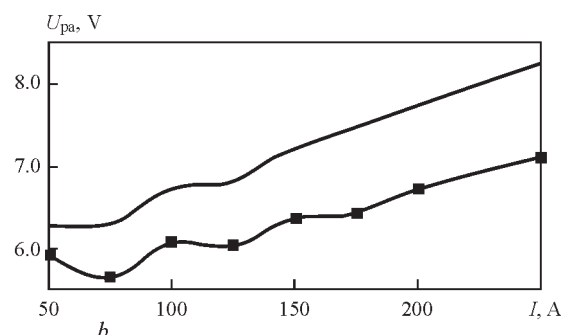


Figure 2. Calculation dependencies of anode potential drop (a) and total voltage on column and anode area (b) on arc current received using model of stationary arc with distributed parameters

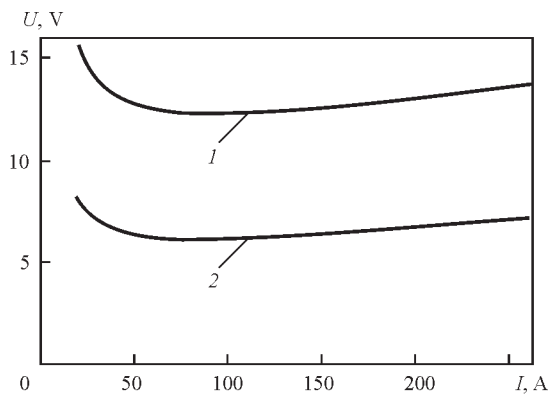


Figure 3. Dependence of arc total voltage (I) (experiment) and sum of effective voltage on column and anode area of arc (2) (calculation) on current

Formula (7) uses a state current concept i_θ which is illustrated employing Figure 5. Only one point of static VAC of $(U_p^{st}(i_\theta), i_\theta)$ coordinates corresponds to each point of dynamic VAC of the arc column with (U_p, I) coordinates. At that, internal energy Q (and resistance R) of the arc column is equal in static and dynamic states.

Formula (7) follows from the equations, which correspond to Kirchhoff laws, describing electric circuit. These equations are complimented by equation of the arc column dynamic model, which is an electro-technical analogue [12] of equation (6):

$$\theta \frac{di_\theta^2}{dt} + i_\theta^2 = I^2. \quad (8)$$

It should be noted that static VAC of arc column can be measured experimentally as well as calculated theoretically using the distributed parameters model.

Total arc voltage was determined by formula

$$U(I) = \frac{U_p^{st}(i_\theta)}{i_\theta} I + U_c(I) + U_a(I), \quad (9)$$

where $U_a(I)$ is the effective anode potential drop, which can be determined employing the distributed parameters model; $U_c(I)$ is the effective cathode

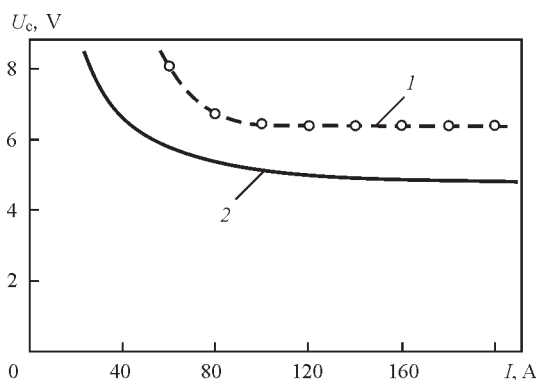


Figure 4. Dependence of cathode voltage drop on arc current: 1 — on data of work [11]; 2 — calculation in accordance with data given in Figure 3

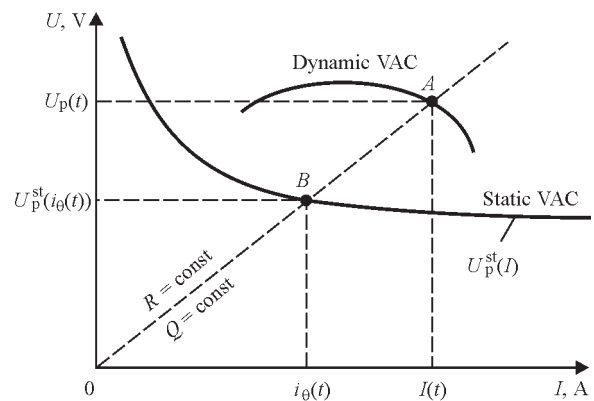


Figure 5. Determination of dynamic arc column voltage drop using concept of arc state current i_θ

potential drop, which can be determined using the proposed calculation-experimental procedure.

Thus, nonstationary arc voltage drop in scope of the dynamic model is calculated as a function of instantaneous value of current in pulse. At that, data on dependence of anode and cathode potential drop on current, which were obtained experimentally or using distributed parameter model, are employed as priori set parameters of the dynamic arc model.

Dynamic VAC of argon arc with refractory cathode. Application algorithm for model with lumped parameters requires its preliminary calibra-

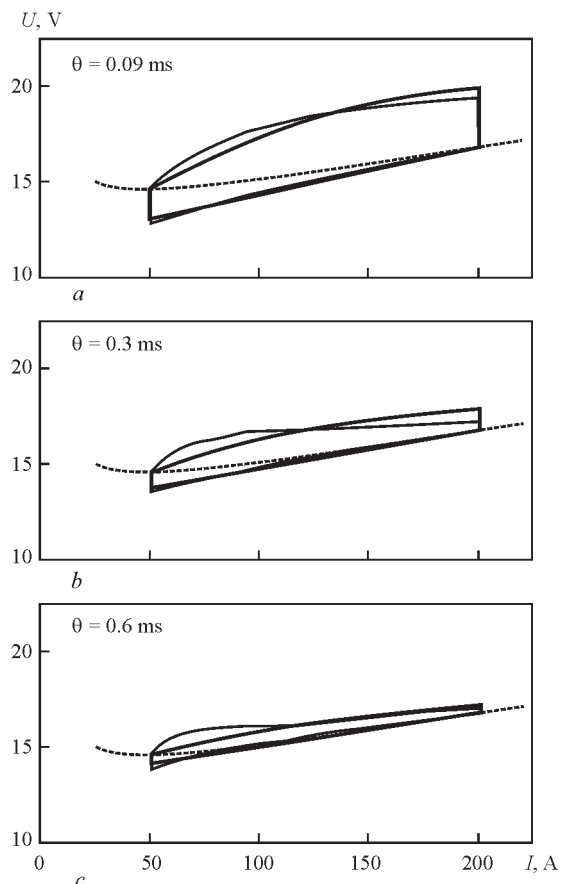


Figure 6. Static (dotted lines) and dynamic VAC of arc model with distributed (solid) and lumped (solid thick) parameters at durations of pulse edges of 20 (a), 100 (b) and 200 (c) μ s

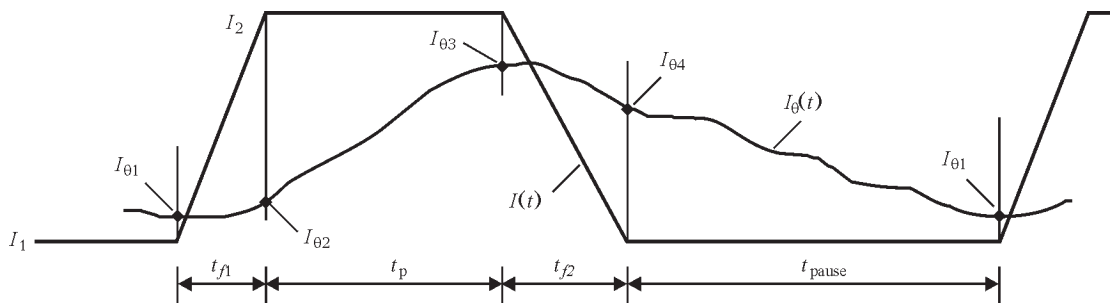


Figure 7. Investigation of influence of trapezoid current pulse on arc using fitting method

tion, namely, determination of time constant θ . For this it is necessary to choose some dynamic mode of arcing, being described by both models and compare their results. Value of the time constant θ can be determined when reaching maximum matching of the results by means of its fitting.

This work studies impact on the arc of trapezoidal pulses of current with different duration of edges. The calculations were carried out for argon arc of 3 mm length with refractory cathode and water-cooled anode. Pulse parameters were varied in the following way: duration of leading and trailing edges of pulse were 20, 100 and 200 μ s. It is assumed that after current increase (drop) the arc burns at direct current, corresponding to the end of transition process up to setting of stationary state. The cathode and anode potential drops depending on instantaneous current value were selected in correspondence with data of Figures 2 and 4. The results of calculation of dynamic VAC for the models with distributed parameters are presented in Figure 6.

Below is given a brief description on calculation of the dynamic VAC employing arc model with lumped parameters in supply of trapezoid current pulse (Figure 7).

Such an impact can be studied stepwise, as a sequential effect of pulse edges (of t_{f1} and t_{f2} durations) and direct current (of t_p and t_{pause} pulse durations). General solutions of differential equation (8) for these steps are as follows:

$$i_{\theta C}^2(t, I_{\theta}, I_1) = I_1^2 + (I_{\theta}^2 - I_1^2)e^{-t/\theta}; \quad (10)$$

$$i_{\theta f}^2(t, I_{\theta}, I_1, I_2, t_f) = I_{\theta}^2 e^{-t/\theta} + I_1^2 (1 - e^{-t/\theta}) - 2 \frac{\theta}{t_f} I_1 (I_2 - I_1) \left(1 - \frac{t}{\theta} - e^{-t/\theta} \right) + 2 \left(\frac{\theta}{t_f} \right)^2 \left(1 - \frac{t}{\theta} + \frac{t^2}{2\theta^2} - e^{-t/\theta} \right), \quad (11)$$

where t_f is the edge duration; I_{θ} is the initial value of state current at each step.

Stationary solutions were found by fitting method, which allowed determining conditions on edge boundaries:

$$\begin{aligned} i_{\theta f} (t_{f1}, I_{\theta1}, I_1, I_2, t_{f1}) &= I_{\theta2}; \\ i_{\theta C} (t_p, I_{\theta2}, I_2) &= I_{\theta3}; \\ i_{\theta f} (t_{f2}, I_{\theta3}, I_2, I_1, t_{f2}) &= I_{\theta4}; \\ i_{\theta C} (t_{\text{pause}}, I_{\theta4}, I_1) &= I_{\theta1}. \end{aligned} \quad (12)$$

Solutions of equations (12) become compact due to matrix recording form:

$$\begin{pmatrix} I_{\theta1}^2 \\ I_{\theta2}^2 \\ I_{\theta3}^2 \\ I_{\theta4}^2 \end{pmatrix} = \begin{pmatrix} -e^{-t_{f1}/\theta} & 1 & 0 & 0 \\ 0 & -e^{-t_p/\theta} & 1 & 0 \\ 0 & 0 & -e^{-t_{f2}/\theta} & 0 \\ 1 & 0 & 0 & -e^{-t_{\text{pause}}/\theta} \end{pmatrix}^{-1} \times \begin{pmatrix} i_{\theta f}^2(t_{f1}, 0, I_1, I_2, t_{f1}) \\ i_{\theta C}^2(t_p, 0, I_2) \\ i_{\theta f}^2(t_{f2}, 0, I_2, I_1, t_{f2}) \\ i_{\theta C}^2(t_{\text{pause}}, 0, I_1) \end{pmatrix}. \quad (13)$$

Substitution of values of state currents on the boundaries of these stages from formula (13) in expressions (10) and (11) allows receiving a dependence of change of state current on time under effect of trapezoid pulse on arc.

If duration of pulse and pause are taken sufficiently large (for arc to reach stationary state), the results received employing lumped parameters can be compared with the results obtained for single edges (see Figure 6) using the model with distributed parameters.

Values of time constant θ in the model with lumped parameters, received by comparison of two models, are indicated in this Figure. It should be noted that the time constant decreases with reduction of the pulse edge duration. Typical feature of VAC of the dynamic arc is the fact that it is presented in form of hysteresis loop, in which upper and lower curves correspond to leading and trailing pulse edge, and vertical pieces — to transfer in arc stationary state (static VAC is plotted in this Figures for comparison). Dynamic VAC in form of hysteresis loop was experimentally received

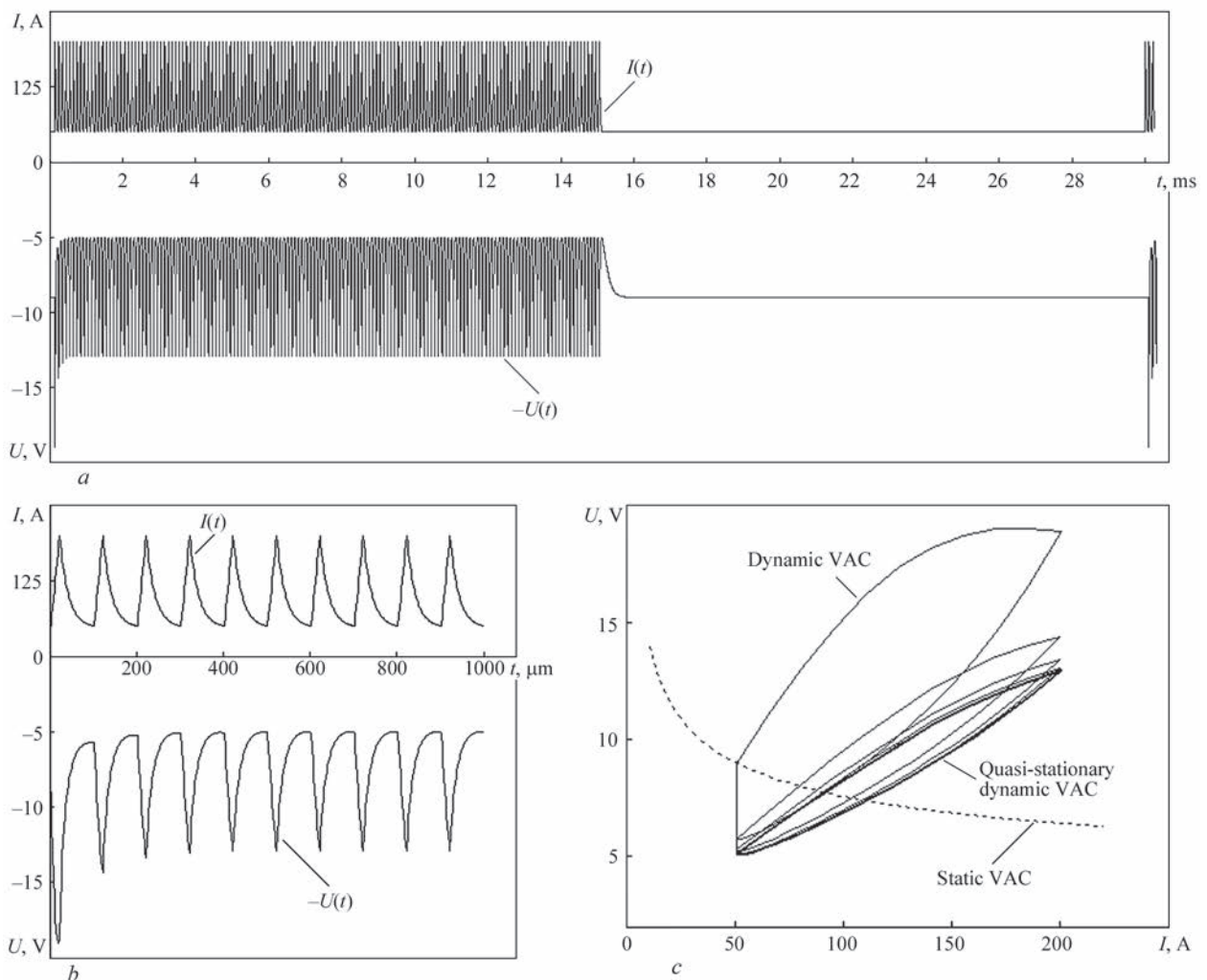


Figure 8. Impact of batches of high-frequency current pulses on arc: *a* — time dependence of arc current and voltage; *b* — influence of several initial pulses of batch (enlarged scale); *c* — calculation dynamic VAC of arc at such an influence

in works [10, 11]. Physical reason of appearance of such a loop is different level of inertia of processes of energy, pulse and charge transfer at current rise or drop [5]. It should be noted that increase of pulse duration promotes for reduction of spread of hysteresis loop and VAC of the dynamic arc is approached to VAC of the static arc.

After finalizing the model of dynamic arc with lumped parameters, above described, and calibrating the time constant, this model was used for calculation of the dynamic VAC in supply of batches of HF pulses. In experimental way pulses were generated using a device, developed in the PWI Department. This device generates batches of HF pulses in 5–25 kHz frequency range of close to triangular form. Frequency of sequence of pulse batches is 1–75 Hz, filling of batch by HF pulses makes from 1 to 99 %.

Experimental researches of impact of batches of HF pulses on arc were carried out, and oscillograms of change of current and arc voltage in time were received. Theoretical study of the same impact using the lumped parameters model showed (Figure 8) good

matching of the results with the experimental data, that indicates adequacy of the proposed description of transfer processes in the arc at welding current HF modulation. Data of Figure 8, *c* indicate that reaction of the arc for six-eight initial pulses of the batch differ from reaction for the rest of pulses. Quasi-stationary dynamic VAC of the arc is formed only after this transfer process is finished.

Conclusions

A concept of effective values of arc voltage components was implemented, namely the cathode and anode potential drop as well as column voltage, taking into account non-equipotentiality of interfaces of the electric arc column with its near-electrode areas. The effective values of voltage drop on column and anode layer of argon arc with refractory cathode and water-cooled anode were calculated based on the model with distributed parameters. The effective cathode potential drop in such an arc is determined by calculation-experimental method.

It is shown that corresponding selection of the time constant allows sufficiently accurate conformity of the results of calculations of transfer processes in the pulsed arc with refractory cathode, based on the model with lumped parameters, to the calculation data received using the distributed parameters model. The dynamic model of arc with lumped parameters does not require large calculation resources, that make it perspective for investigation of transfer processes in supply of batches of high-frequency pulses.

Volt-ampere characteristics of the arc were received based on comparative analysis of the models with lumped and distributed parameters, describing transfer processes in the pulse arc with refractory cathode. It is shown that increase of slopes of edges of current pulses provides for rise of spread of hysteresis loop of arc dynamic VAC.

Adjustment of quasi-stationary VAC of the pulsed arc with refractory cathode at HF current modulation of arc current is achieved after passing 6–8 pulses.

1. Gurevich, S.M., Zamkov, V.N., Kushnirenko, N.A. (1965) Increase of penetration efficiency of titanium alloys in argon arc welding. *Avtomatich. Svarka*, **9**, 1–4.
2. Yushchenko, K.A., Kovalenko, D.V., Kovalenko, I.V. (2001) Application of activators for TIG welding of steels and alloys. *The Paton Welding J.*, **7**, 37–43.
3. Steen, W.M., Eboo, M. (1979) Arc augmented laser welding. *Metal Construction*, **11**(7), 332–335.
4. Lu, S., Fujii, H., Nogi, K. (2004) Marangoni convection and weld shape variations in Ar–O₂ and Ar–CO₂ shielded GTA welding. *Materials Sci. and Eng. A*, **380**(1/2), 290–297.
5. Krivtsun, I.V., Krikent, I.V., Demchenko, V.F. (2013) Modelling of dynamic characteristics of a pulsed arc with refractory cathode. *The Paton Welding J.*, **7**, 13–23.
6. Krivtsun, I.V., Demchenko, V.F., Krikent, I.V. (2010) Model of the processes of heat-, mass- and charge transfer in the anode region and column of the welding arc with refractory cathode. *Ibid.*, **6**, 2–9.
7. Sanders, N.A., Pfender, E. (1984) Measurement of anode falls and anode heat transfer in atmospheric pressure high intensity arcs. *J. Appl. Phys.*, **55**(3), 714–722.
8. Krikent, I.V., Krivtsun, I.V., Demchenko, V.F. (2012) Modelling of processes of heat-, mass- and electric transfer in column and anode region of arc with refractory cathode. *The Paton Welding J.*, **3**, 2–6.
9. Krikent, I.V., Krivtsun, I.V., Demchenko, V.F. (2014) Simulation of electric arc with refractory cathode and evaporating anode. *Ibid.*, **9**, 17–24.
10. Krivtsun, I.V., Krikent, I.V., Demchenko, V.F. et al. (2015) Interaction of CO₂-laser radiation beam with electric arc plasma in hybrid (laser + TIG) welding. *Ibid.*, **3/4**, 6–15.
11. Uhrlandt, D., Baeva, M., Kozakov, R. et al. (2013) Cathode fall voltage of TIG arcs from a non-equilibrium arc model. In: *IIW Doc. 2500*. SG 212 on Physics of Welding.
12. Sidorets, V.N., Pentegov, I.V. (2013) *Deterministic chaos in nonlinear circuits with electric arc*. Kiev: IAW.
13. Trofimov, N.M., Sinitsky, R.V. (1967) Dynamic characteristics of pulsed arc in argon arc welding. *Svarochn. Proizvodstvo*, **8**, 18–19.
14. Sokolov, O.I., Gladkov, E.A. (1977) Dynamic characteristics of free-burning and constricted welding arcs of direct current with nonconsumable electrode. *Ibid.*, **4**, 3–5.

Received 26.10.2015